Geophys. J. Int. (1989) **99**, 205–222

Syn-deformational remanent magnetization of the Mount Eclipse Sandstone, central Australia

Z. X. Li and C. McA. Powell
Australian Plate Research Group, School of Earth Science, Macquarie University, NSW 2109, *Australia*

P. W. Schmidt
CSIRO Division of Exploration Geoscience, PO Box 136, *North Ryde*, NSW 2113, *Australia*

Accepted 1989 April 14. Received 1989 April 14; in original form 1988 August 26

SUMMARY

The palaeomagnetism of the latest Devonian–Early Carboniferous Mount Eclipse Sandstone in central Australia reveals samples from 16 out of 31 sites having a consistent high-temperature component of natural remanent magnetization. Site-mean directions from the two limbs of the most detailed studied syncline attain their best grouping after 75 per cent of 'unfolding', and further 'unfolding' causes a 'cross-over' feature. Mineralogical studies using microscope and electron microprobe show that this remanance is most likely to be carried by secondary haematite formed by alteration of Fe-rich minerals during the mid-Carboniferous deformation. Four different models are examined to reconstruct the palaeo-horizontal for the syn-deformational remanence. The best estimate of the palaeomagnetic South Pole position is lat. = 33.8°S, and long. = 121.2°E (dp = 19.2°, dm = 19.7°), close to Australia. This result indicates a rapid polarward movement of eastern Gondwanaland during the first half of the Carboniferous. We also suggest that the widespread Alice Springs Orogeny-related overprints in central Australia were acquired during the beginning of the main phase of deformation in the mid-Carboniferous.

Key words: Carboniferous, Gondwanaland, overprint, palaeomagnetism, Pangaea, syn-deformational

1 INTRODUCTION

The hypothesis that the supercontinent of Gondwanaland moved across the South Pole between the Early Carboniferous and the mid-Permian was first proposed by Köppen & Wegener (1924) in order to explain the migration of a continental glaciation centre from Africa to Australia during the Late Palaeozoic, and was supported by many later palaeoclimatologists (e.g. King 1962; Crowell 1978; Caputo & Crowell 1985) and palaeontologists (e.g. Runnegar & Campbell 1976). But, since the onset of ice ages is related to many factors other than the palaeolatitudes of continental masses, e.g. continent–ocean distribution and orogenic uplift in continental masses, (Crowell 1978; Powell & Veevers 1987; Veevers & Powell 1987), details of when this movement occurred, within the ~90 Ma interval, are still unclear. To define the latitudinal movement quantitatively, palaeomagnetic work on Late Palaeozoic rocks from Australia has been carried out by many workers (Irving & Parry 1963; Irving 1966; Chamalaun & Porath 1968; Hurley & Van der Voo 1987; Schmidt *et al.* 1986; Li, Schmidt & Embleton 1988). All these data, however, correspond to one of two age groups: Late Devonian–earliest Carboniferous and Permo-Carboniferous. Reliable data for the key period, the mid-Carboniferous, are non-existent. Therefore, this work was designed to obtain some palaeomagnetic data of Early to mid-Carboniferous age from cratonic Australia which could be used to derive a reference pole and thus refine further Gondwanaland's Late Palaeozoic drift history.

2 REGIONAL GEOLOGY AND SAMPLING

The Ngalia Basin is an asymmetrically faulted structural basin in central Australia (Fig. 1a), with its basement gently tilted to the north. It comprises Adelaidean (Late Proterozoic) and Palaeozoic sediments with a thickness of up to 5 km, deposited on the Precambrian granitic, gneissic and charnockitic basement. At various stages through its history, the sediments of the Ngalia Basin were probably connected with sediments of the Amadeus Basin to the south, and to other areas to the north and west.

The Mount Eclipse Sandstone is the youngest Palaeozoic sedimentary unit in the basin and unconformably overlies most of the older rocks. It consists of coarse-grained arkosic sandstone and subgreywacke with interbedded conglomerate, subordinate red siltstone, and shale. The colour of the

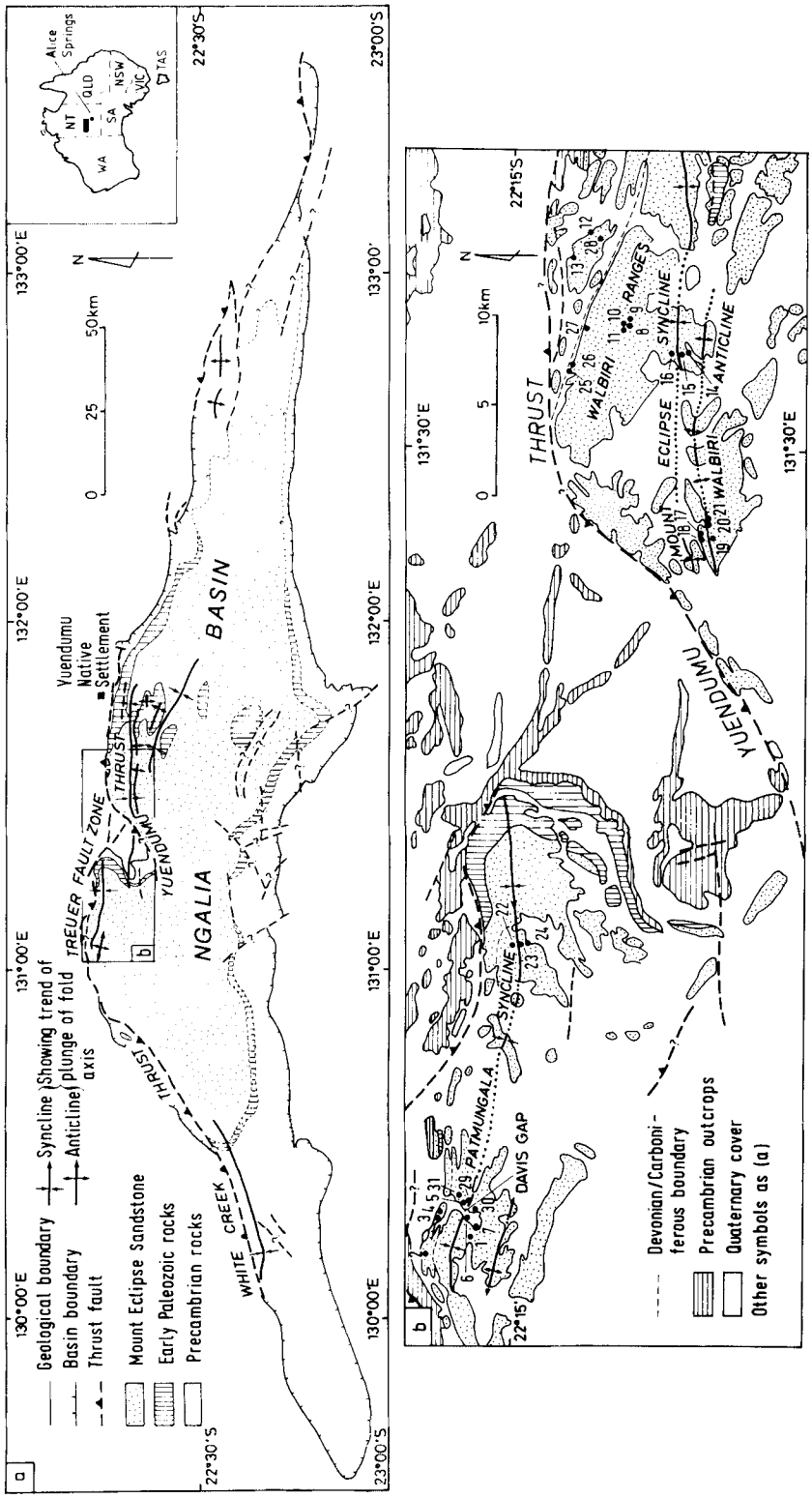

Figure 1. (a) Structural pattern of the Ngalia Basin and (b) the sampling localities.

sandstone varies locally from white to reddish brown or brick red, whereas the colour of all outcropping siltstones is red. The total thickness of this formation, estimated from the Walbiri Ranges region (Fig. 1b), is about 3700 m.

The age of the Mount Eclipse Sandstone ranges from latest Devonian to mid-Carboniferous. Based on palaeontological evidence (Wells & Moss 1983; D. G. Morris, pers. comm.), the Devonian–Carboniferous boundary can be mapped in the Davis Gap area (Fig. 1b), where it is marked by a palaeosoil unit. This unit is recessive, and it is marked on aerial photographs by a change in the character of the outcropping sandstone bands. The Famennian rocks outcrop as rather thick, knobbly lenses, whereas the overlying Lower Carboniferous rocks are thinner-bedded and form laterally continuous bands, commonly arranged in upward-thinning cycles. The Devonian–Carboniferous boundary is extrapolated to lie in the Mount Eclipse region by the authors based on the boundary's relative position in the formation and airphoto interpretation. A generalized stratigraphic column of the formation is shown in Fig. 2.

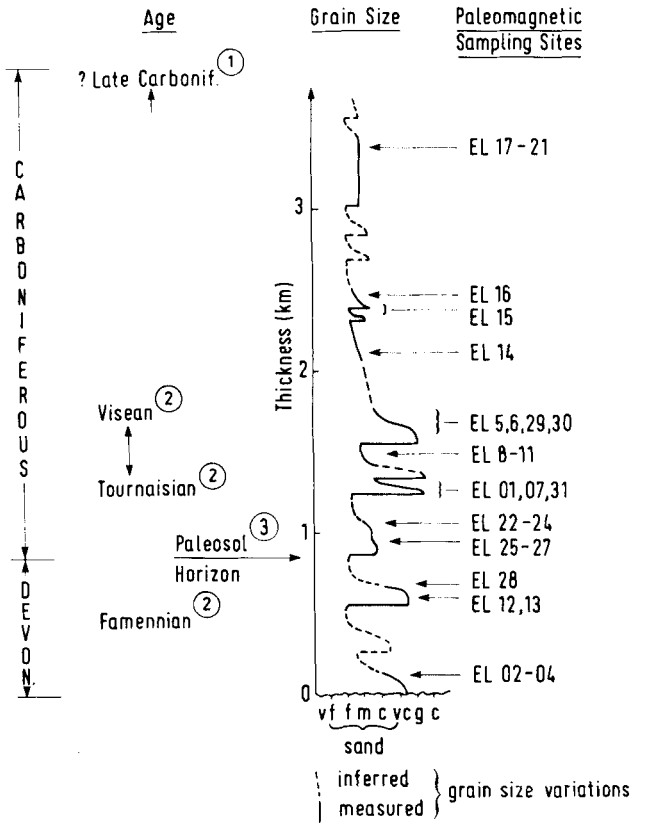

Figure 2. Schematic diagram showing the age, the grain-size distribution, and the stratigraphic positions of the sampling sites. The total thickness of the formation is estimated from the air photographs of the Walbiri Range region in combination with bedding attitudes measured in the field and also taken from the regional geological map (Australia 1:250,000 Geological Series, Mount Doreen sheet, published by the Bureau of Mineral Resources, Canberra, 1972). The age assignations are adopted from: 1, Appendix 6 in Wells & Moss (1983); 2, R. Evans, G. Playford & E. M. Truswell in Saucier 1981, unpublished work; 3, D. G. Morris, pers. comm.

Table 1. Bedding and localities of the sampling sites

Fold	Site	Zone Age	n	Bedding So	n'	a95	Location Lat (°S)	long (°E)
	EL01	C_1	14	24.2/020.6	7	4.9	22.24	131.08
	EL02	D_3	18	78.4/018.8*	8	3.5	22.21	131.07
	EL03	D_3	13	74.1/203.0	6	4.3	22.22	131.09
	EL04	D_3	17	71.6/198.2	7	3.9	22.22	131.09
Patmungala	EL05	C_1	18	73.3/198.4	6	2.9	22.23	131.09
	EL06	C_1	23	40.4/014.1	12	3.1	22.23	131.08
Syncline	EL07	C_1	10	20.5/025.1	6	3.0	22.24	131.08
	EL29	C_1	15	68.2/200.5	4	3.0	22.23	131.09
	EL30	C_1	14	38.8/020.4	5	4.6	22.24	131.09
	EL31	C_1	14	74.6/196.5	3	5.2	22.23	131.10
	EL22	C_1	15	28.0/217.9	8	3.9	22.23	131.23
	EL23	C_1	11	21.2/255.8	4	1.2	22.23	131.23
	EL24	C_1	10	9/317	1		22.24	131.23
	EL08	C_1	8	21.5/211.6	7	2.5	22.31	131.57
	EL09	C_1	6	same			22.31	131.57
	EL10	C_1	7	21.8/207.0	6	2.4	22.31	131.57
	EL11	C_1	9	same			22.31	131.57
Mount	EL12	D_3(?)	12	11.4/233.6	8	2.5	22.29	131.61
	EL13	D_3(?)	10	9.0/215.4	8	2.7	22.28	131.60
Eclipse	EL14	C_1	12	45.2/347.6	9	2.7	22.34	131.55
	EL15	C_1	8	same			22.33	131.55
Syncline	EL16	C_1	9	13.3/266.6	4	3.0	22.33	131.55
	EL25	C_1	9	30.9/219.3	6	3.3	22.28	131.54
	EL26	C_1	8	45.2/209.0	4	4.6	22.28	131.54
	EL27	C_1	14	26.5/196.4	4	2.7	22.29	131.56
	EL28	D_3(?)	15	11/206	1		22.29	131.61
	EL17	C_1	9	45.8/339.5	6	3.8	22.34	131.46
Walbiri	EL18	C_1	11	same			22.34	131.46
	EL19	C_1	13	47.6/186.6	8	2.3	22.35	131.45
Anticline	EL20	C_1	8	12.9/208.6	9	3.0	22.35	131.46
	EL21	C_1	13	same			22.35	131.46

D_3 - Late Devonian; C_1 - Early Carboniferous; n - number of samples collected; So - bedding orientation shown by dip/dip-azimuth; n' - number of bedding mesurements; a_{95} - half angle of the 95% confidence cone; * - bedding overturned.

The Mount Eclipse Sandstone, together with the underlying rocks, was deformed during the mid-Carboniferous Mount Eclipse movement (i.e. the latest stage of the Alice Springs Orogeny), which was the strongest movement in this region since the Precambrian. The intensity of deformation increases from south to north. Thrusts or high-angle reverse faults mark the northern margin of the Ngalia structural basin with displacement on low-angle faults of at least 10 km in places (Wells & Moss 1983).

Sampling was concentrated in the northern part of the basin where the Mount Eclipse Sandstone is well exposed and was moderately to strongly folded (Fig. 1b). Outcrop is very poor in the southern part of the basin, which is known mainly from drill cores. A total of 373 orientated core samples were collected from 31 sites in the Mount Eclipse Sandstone using a portable drill. More than five bedding measurements were taken at most of the sites, and a mean bedding orientation ($\alpha_{95} < 5°$, see Table 1) was used in structural correction. Samples were taken from both the uppermost Devonian part of the formation (sites EL02, 03, 04, 12, 13, 28) and the Lower Carboniferous part (all other sites, see Fig. 2). Attention was paid to locate sites on both limbs of folds so that a fold test, as discussed by Graham (1949) and McFadden & Jones (1981), might be applied. In order to avoid local structural complications which would involve complex rotations, sampling sites were all located in areas where the local fold axes conformed with the regional east–west structural trend. The fold hinges are generally horizontal. Only at the noses of the folds minor (up to 10°) tilts are observed.

3 LABORATORY TECHNIQUE

Two or three cylindrical core specimens of 25 mm diameter and 22 mm height were cut from each sample. A non-magnetic automatic furnace within a magnetic-free space (~±5 nT) (Coward *et al.* 1985) and a Schonstedt GSD-1 alternating magnetic field (AF) demagnetizer were employed for demagnetizing the specimens. A shielded three-axis CTF cryogenic magnetometer, housed inside a set of three orthogonal Helmholtz coils, was used for remanence measurements.

Generally two specimens from each sample were demagnetized. Up to 12–13 demagnetizing steps were applied to pilot specimens; to the bulk of the remaining specimens 6–10 steps were applied. AF demagnetization up to 55 mT (550 Oe) was tried on some specimens from the Davis Gap area and was found to be ineffective, except for a few specimens from site EL06. Further thermal demagnetization was carried on these specimens. Only stepwise thermal demagnetization was applied to the rest of the specimens, with temperatures starting from 60 °C up to a maximum of 680 °C. All the data were presented as orthogonal vector plots (Zijderveld 1967), and vector components of natural remanent magnetization (NRM) were identified using principal component analysis (Kirschvink 1980). Behaviour between specimens was not consistent enough to use linearity spectrum analysis (LSA, Schmidt 1982). Site-mean directions were calculated for the samples exhibiting stable remanence and no inconsistency between specimens. Outlying remanence directions identified by eye were excluded from this calculation. For final data analysis, only site-mean directions based on at least three sample-means, with α_{95} less than 30°, were used. To help with data interpretation, a preliminary mineralogical study was undertaken using a transmitting optical microscope and an electron microprobe.

4 RESULTS AND DATA INTERPRETATION

The NRM intensity of the samples was very low, generally varying from less than 1 mAm^{-1} (1.0×10^{-6} emu cm^{-3}) to 2–3 mAm^{-1}, although in some instances intensity of up to a few tens of mAm^{-1} was observed. Seventy-six out of the 373 samples failed to reveal any characteristic remanence. Data from these samples were discarded from further analysis.

Orthogonal plots of some typical demagnetization data are given in Figs 3 and 4. Two characteristic remanent magnetization components were identified. One is a low-temperature component (L) with unblocking temperatures of less than 200 °C and a coercivity of about 30 mT (300 Oe). The other is a high-temperature component (H) with unblocking temperatures distributed from about 200 °C up to more than 650 °C. Most of the high-temperature components decay approximately towards the origin in their vector plots (Fig. 3a–h), although some are clearly offset from the origin (Fig. 3i). The highest stability component was not resolved. Also, in a few other specimens an intermediate linear segment is observed (Fig. 4a, b), but as shown in stereoplots (Fig. 4c, d), such linear segments lie within the plane containing the characteristic low-temperature and high-temperature components, suggesting that these linear segments are 'pseudo-segments' and should be interpreted as combinations of the two principal components discussed above.

The low-temperature component could be carried either by very fine-grained haematite or by goethite (Strangway *et al.* 1968), but the high-temperature component is probably carried by haematite as suggested by its high unblocking temperature and high coercivity. This conclusion is also supported by the magnetic mineralogy study (see Section 5).

Fig. 5 shows the stereographic plots of the sample-mean directions of the high-temperature component for sites which satisfied the selection criteria after excluding no more than two outliers from each site. The samples from most of the sites were found to be reversely magnetized relative to the generally accepted apparent polar wander path (APWP) for Gondwanaland, but samples from some sites were found to carry both normal and reversed polarity. For sites with mixed polarities, sample-mean directions were all converted to the dominant polarity before calculating the site-mean directions. The accepted site-mean directions of both the low- and high-temperature components are listed in Table 2. Since the sampling spread is only about 60 km in extent, the effect of the locality difference on the direction of the geomagnetic field is small enough to be ignored during data analysis.

Fig. 6 shows that the *in situ* site-mean directions for the low-temperature component cluster around the direction of the present geomagnetic field (P) and the dipole field (D), but become dispersed after bedding correction. Considering its consistent normal polarity and low unblocking temperature, this component is interpreted as a viscous remanent magnetization (VRM) acquired during the Brunhes normal polarity interval (<0.73 Ma).

The interpretation of the high-temperature component is more ambiguous than for the low-temperature one. Fold tests were applied to these data in order to define the age and the palaeohorizontal pertaining to the magnetization. The data from the Carboniferous section of the formation in the Davis Gap area (sites EL01, 05, 06, 07, 29, 30, 31) appeared initially to be most suited to a fold test, so they are considered first.

4.1 Cross-over feature of magnetization in the Lower Carboniferous rocks of Davis Gap area

The mean directions of these sites are plotted in Fig. 7a, which shows that although data from the two fold limbs are much better grouped after bedding correction, there is clearly a 'cross-over' during the bedding correction. Assuming data from the two limbs were originally drawn from the same Fisher distribution (Fisher 1953), the hypothesis that they share a common mean direction was tested at different stages of bedding correction using the method given by McFadden & Jones (1981). According to McFadden & Jones, if we assign the northern limb label **a**, and the southern limb label **b**, we have

$$M = 1 - \left(\frac{Ra + Rb - R^2/(Ra + Rb)}{2(N - Ra - Rb)} + 1\right)^{(2-N)} \quad (1)$$

where M is the significance level at which the above hypothesis can be rejected, Ra and Rb are the resultant

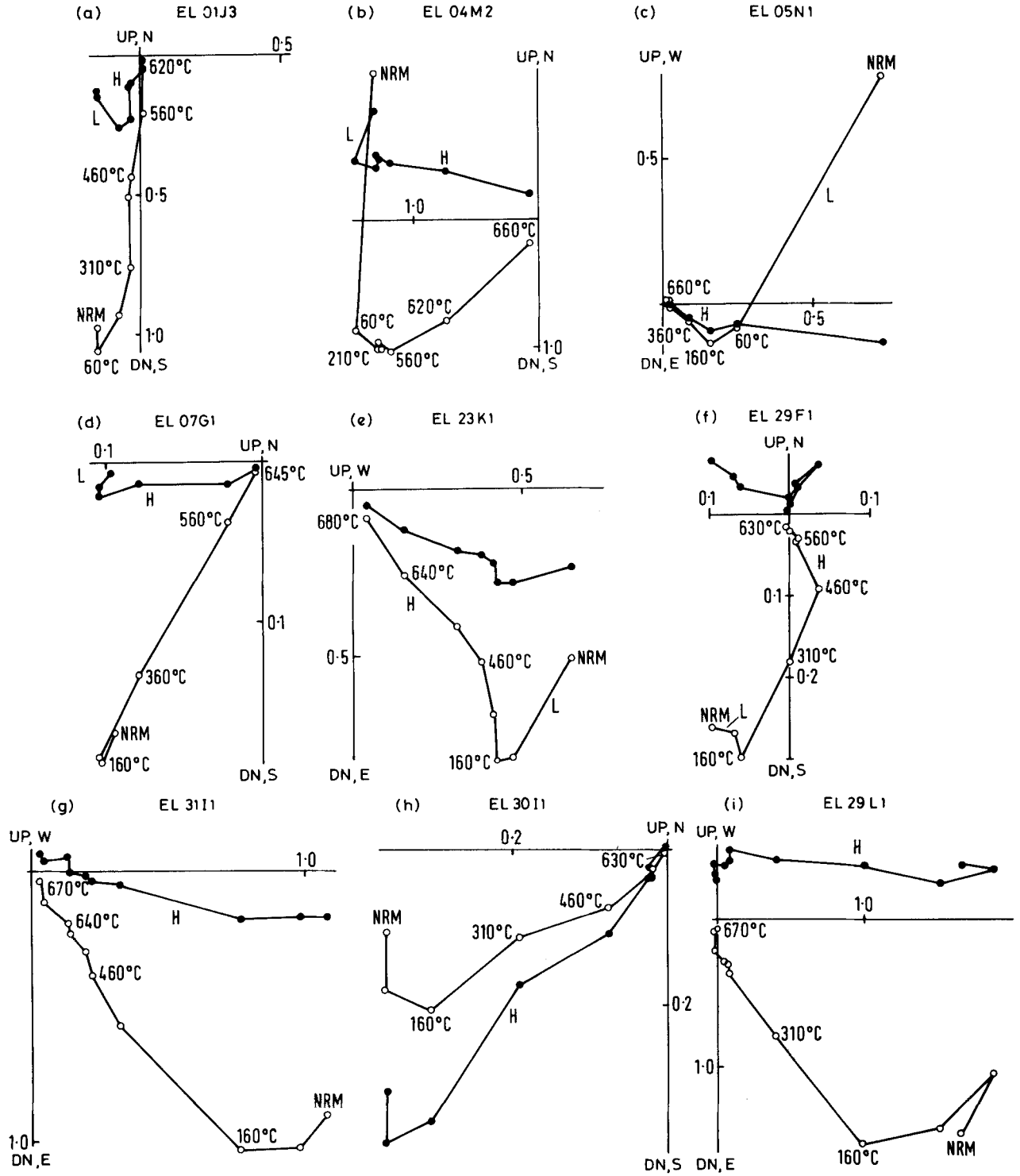

Figure 3. Representative orthogonal plots of magnetization vectors revealed by thermal demagnetization. Solid (open) circles are projections on horizontal (vertical) planes. The unit of intensity on the plots is mAm^{-1}. H stands for the high-temperature characteristic remanence, and L stands for the low-temperature recent overprint component. Data are shown before bedding correction.

lengths of the site-mean unit vectors from limb **a** and limb **b**, and R is that of both limbs, N being the total number of sites. Figure 8a plots the change of M and the estimate of the Fisher precision parameter k during proportional stepwise 'unfolding'. This shows that the hypothesis of the two groups of site-mean directions sharing a common mean direction can be rejected at significance levels of greater than 95 per cent both before 55 per cent and after 90 per cent of 'unfolding'. M and k reach their minimum and maximum values, respectively, at about 75 per cent of 'unfolding'.

The cross-over feature of remanent directions during

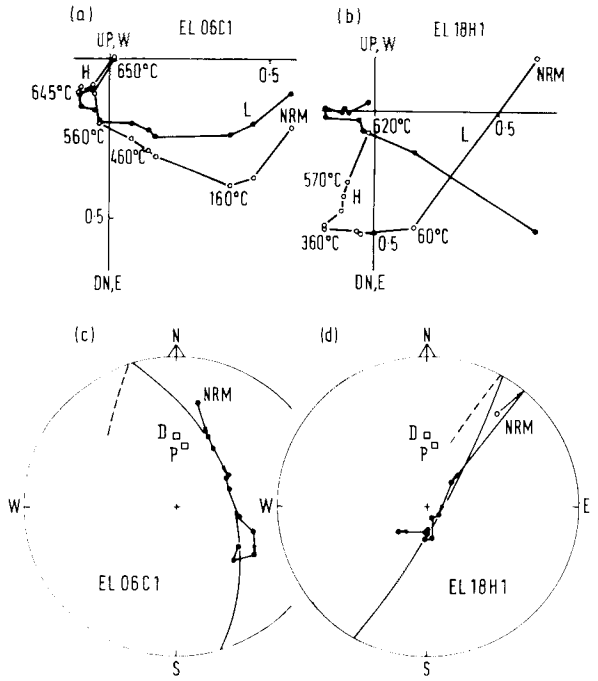

Figure 4. Orthogonal plots (a and b) of two specimens with a typical intermediate linear segment. (c) and (d) show that all the remanence vectors from the specimens in (a) and (b) fall close to a great circle, which connects the characteristic low-temperature and high-temperature components. Projection and symbols in (a) and (b) are the same as in Fig. 3. Solid (open) symbols in (c) and (d) are equal-angle projections on the lower (upper) hemisphere. (P) and (D) represent the local directions of the present and dipole magnetic fields.

bedding correction has been reported for other rock units by many workers in the last few years (Perroud, 1983; McClelland Brown 1983; Schwartz & Van der Voo 1984; Kent & Opdyke 1985; Schmidt & Embleton 1985; Granrer, Burmester & Beck 1986; Miller & Kent 1986; Torsvik *et al.* 1986). It has been mostly regarded as an indicator of syn-deformational remanent magnetization, although some studies (Facer 1983; Spariosu, Kent & Keppie 1984; Kodama 1986a,b; Van der Pluijm 1987) have suggested that it could be the result of internal strain of a pre-deformational remanent magnetization. Although pressure solution and deformation lamellae are common in the rocks we studied, there are very few depositional magnetic grains in these rocks (details are reported in Section 5 of this paper). We prefer to interpret the above remanence as a syn-deformational remanent magnetization, which is carried by secondary haematite formed during deformation.

Proportional stepwise 'unfolding', referred to as model A as used for Fig. 8a, has been applied by previous workers (e.g. Perroud 1983; McClelland Brown 1983; Schwartz & Van der Voo 1984) to obtain the correct palaeohorizontal. This proportional bedding-correction process is based on the assumption that the ratio of the tilt angles of the two limbs remains consistent during the deformation. Using this model, the populations from limbs **a** and **b** attain their best grouping when the fold is 'restored' to an open but asymmetric syncline (Table 3, model A). Model A yields a mean tilt-corrected direction of $D = 273.6°$, $I = 82.6°$, $k = 62.3$, $\alpha_{95} = 7.7°$ for the seven sites.

In the Davis Gap area, although the fold axis is close to horizontal, the fold is strongly asymmetric. Thus, an alternative model (model B) has been applied for the incremental bedding-correction, which assumes that the Patmungala syncline was symmetric when it acquired the magnetization, and that further folding accompanied by strong thrusting, produced the strongly asymmetric syncline. In model B, the steeper northern limb was partially corrected first to form a symmetric fold, and then the two limbs were 'untilted' synchronously until the site mean directions attained the best grouped Fisher distribution. A mean direction is thus obtained of $D = 244.8°$, $I = 80.0°$, $k = 55.3$, $\alpha_{95} = 8.2°$ when both limbs dip at about 12° (Table 3, model B). Note that k and α_{95} in the two models are not precisely the same because the partial 'unfoldings' were calculated at 5 per cent increments instead of continuously.

Although the difference between models A and B is small, we favour model B because it is consistent with our regional structural analysis. Model A implies that the folding and thrusting occurred synchronously, whereas model B implies that thrusting on the northern limb of the Patmungala syncline was concentrated in the late stage of deformation. We consider that an early stage of regional gentle, symmetric folding (possibly accompanied by some local thrusting), was followed by major thrusting on the northern margin of the Ngalia Basin.

The suggested two-stage pattern of the deformation in model B is supported by the regional structural pattern. In the Ngalia Basin, truncations of fold hinges by thrusts, and bending of regional fold hinges adjacent to thrusts are common both in the map pattern (Fig. 1) and in the seismic reflection profile interpretation (Wells & Moss 1983, plate 2). In the Patmungala Syncline, the bedding in the northern limb varies from very steep and upright to overturned, whereas the bedding in the southern limb has a uniform dip to the north of only about 30°. The distribution of the overturned bedding is specifically related to proximity to the basement-rooted thrust along the present northern edge of the Ngalia Basin. It is thus reasonable to infer that the strong tilting of the northern limb of the Patmungala Syncline was related to the growth of thrusts late in the deformation sequence.

Two extreme cases (models C and D) can be obtained in which one limb is assumed to be horizontal when magnetized while the other was tilted. Although there is no independent evidence to support these two models, they are nevertheless useful in constraining the possible position of the palaeomagnetic pole. The least dispersed mean directions of each of the four models discussed are listed in Table 3.

4.2 Combined interpretation of all other accepted sites

Figure 7(b) plots the site-mean directions of the uppermost Devonian rocks in the Mount Eclipse Sandstone both before and after bedding correction. It clearly shows that the mean directions from these sites become much more dispersed after bedding correction, indicating that the magnetization could not be a pre-deformational remanence. The limited number of sites made it difficult to estimate the precise palaeohorizontal for this remanence. However, two out of the three site-mean directions pass the best estimated

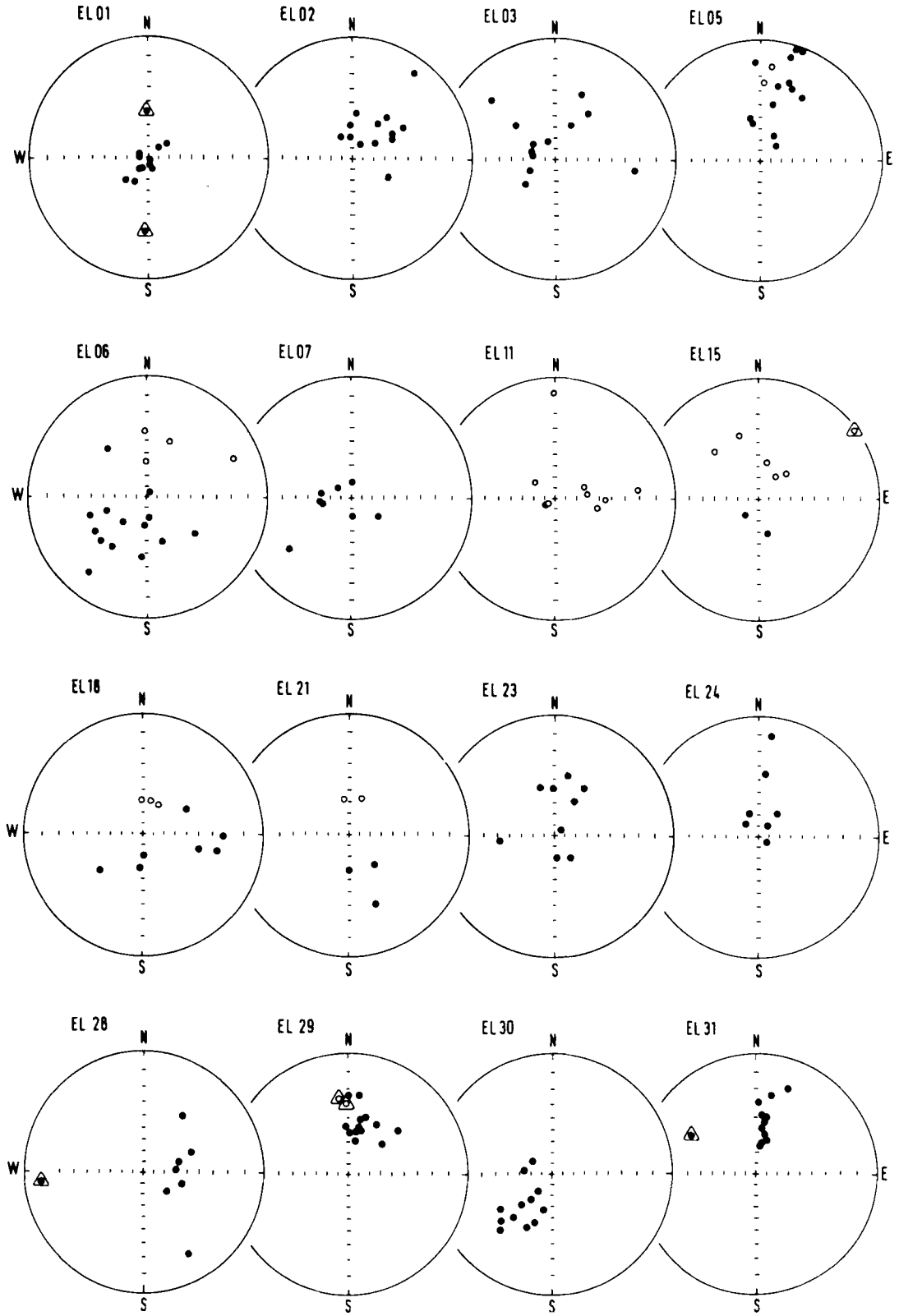

Figure 5. Equal-angle projection of high-temperature component directions from all sites for which the data satisfy our selection criteria. Each data point represents one sample-mean remanence component direction. Solid (open) circles are projections on the lower (upper) hemisphere. Directions with triangles are outliers.

Table 2. Site mean directions of the remanent magnetisations

Site	Low Temperature Component					High Temperature Component					
	D	I	n	k	a_{95}	D	I	P	n	k	a_{95}
EL01						207.4	82.4	R	11	27.7	8.8
EL02	015.0	-41.7	13	52.5	5.8	040.8	59.0	R	13	9.4	14.3
EL03	008.7	-49.2	8	18.4	13.3	330.4	70.5	R	12	4.2	24.2
EL04	005.0	-42.3	9	27.9	9.9						
EL05	006.4	-41.1	8	35.5	9.4	013.6	26.2	R	15	7.0	15.5
EL06	345.2	-56.4	5	12.9	22.1	212.1	50.2	M	18	5.6	16.1
EL07	356.6	-27.0	8	20.4	12.6	242.7	71.1	R	8	7.8	21.2
EL08	005.7	-49.1	5	17.1	19.0						
EL11	356.4	-41.8	5	25.6	15.4	062.4	-63.8	M	9	4.9	25.9
EL12	035.8	-47.1	6	18.7	15.9						
EL14	001.4	-37.4	7	9.1	21.2						
EL15						012.6	-52.4	M	7	6.2	24.2
EL16	018.0	-44.5	5	9.2	26.7						
EL18	023.3	-33.0	3	79.7	13.9	144.8	62.6	M	10	4.6	25.3
EL19	017.4	-44.1	6	11.2	20.9						
EL20	011.3	-31.7	3	20.9	27.7						
EL21	034.3	-36.6	7	5.7	27.6	169.9	51.5	M	5	19.5	17.8
EL23	343.3	-48.6	5	116.2	7.1	005.7	70.8	R	9	5.1	25.3
EL24	355.3	-43.0	5	89.2	8.1	008.4	64.1	R	7	7.1	24.3
EL26	009.6	-51.2	4	43.7	14.1						
EL27	356.3	-51.0	7	17.5	14.9						
EL28	019.3	-33.1	11	15.5	12.0	094.0	53.7	R	7	6.3	26.2
EL29	356.0	-37.5	11	34.3	7.9	015.9	44.6	R	13	25.5	8.4
EL30	356.4	-47.7	6	64.2	8.4	223.2	49.4	R	12	13.4	12.3
EL31	357.2	-40.0	7	12.3	18.0	009.7	44.8	R	11	24.4	9.4

D - declination; I - inclination; n - number of samples taken into calculation; k - precision parameter of the Fisher distribution; a_{95} - half angle of the 95% confidence cone. P - polarity, where N for normal, R for reversed, and M for mixed. All directions are *in situ*.

direction from the Lower Carboniferous rocks in the Davis Gap area (model B). Further, considering the similarities in mineralogy and structural location of these sites with the Lower Carboniferous ones, we suggest that these rocks have probably acquired their remanent magnetization during the deformation too, at about the same time as the overlying Carboniferous rocks in the Davis Gap area.

Fold tests were also attempted for the Carboniferous samples from the Mount Eclipse Syncline, the Walbiri Anticline and the eastern hinge of the Patmungala Syncline. Because there are only two sites accepted from each of these folds, and the α_{95} of these site-mean directions are usually as large as 25°, fold tests on each fold are inconclusive (Figs 7c–e). However, if we do stepwise 'untilting' on these data and those from the uppermost Devonian rocks, and combine each set of the partially bedding-corrected data with the best grouped (75 per cent 'unfolded') data from the Carboniferous Davis Gap rocks, the overall mean direction attains its greatest Fisher precision parameter after 30–40 per cent 'untilting' (Fig. 7f and Fig. 8b). This suggests that probably all the rocks close to the northern margin of the Ngalia Basin acquired their dominant remanent magnetization during the deformation. Mean directions and corresponding palaeopoles calculated according to each of the four models are listed in Table 3.

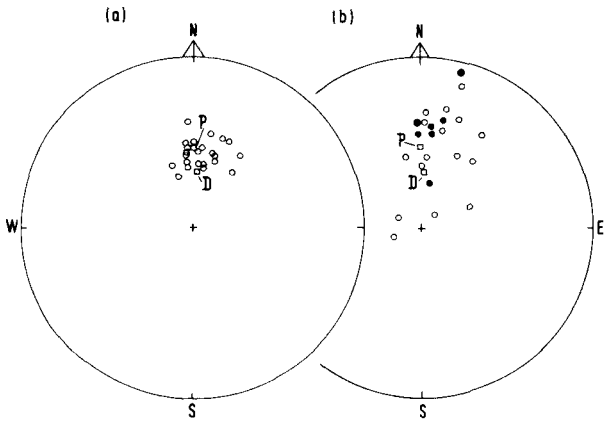

Figure 6. Equal-angle projection of the site-mean directions of the low-temperature component before (a) and after (b) bedding correction. Conventions are the same as in Figs 4 and 5. P = present geomagnetic field direction; D = dipole field direction.

5 SOME MINERALOGICAL OBSERVATIONS

To appraise the syn-deformational model of the magnetization, a preliminary mineralogical study of the samples was carried out. Thin sections from each site were first examined under a microscope using transmitted light, and then six polished thin sections representing the three main sampled areas were analysed using an electron microprobe to identify the opaque minerals in them. For the purpose of this paper, the petrological study concentrated on estimating the degree of deformation and determining how the magnetic remanence carriers relate to the deformation.

Almost all of the thin sections show strong pressure-solution suturing of quartz-grain boundaries (Fig. 9). In places, recrystallization with growth of new quartz grains is found. Fine deformation lamellae closely related to the grain-to-grain contacts are seen in many quartz grains (Fig. 9a, b). Biotite and muscovite occur as detrital phases in all the thin sections, and account for no more than 1 per cent of the total volume. These phyllosilicates are commonly kinked between other detrital grains (Fig. 9e, f). The micas range from very fresh to severely altered.

Iron-oxide minerals in these rocks can be classified into three types according to their occurrence: A, opaque detrital grains; B, red coating on quartz grains, formed during early diagenesis of the rock; and C, red pigment formed after the major grain-scale deformation. The significance of each of these to the remanent magnetization is discussed below.

5.1 Type A, detrital opaque minerals

Detrital opaque minerals appear in all the thin sections, but their total volume is only small. Their grain size generally ranges between 50 and 100 μm. Electron microprobe analysis of the six representative samples revealed that, except for the sample from site EL28, the opaque minerals are all Ti-Fe oxides with their $TiO_2/FeO > 40$ per cent. Because of the impurity of the minerals, the FeO/Fe_2O_3 ratio could not be precisely determined, and the data are presented in Fig. 10 using the TiO_2/FeO ratio only. The intersections of the horizontal lines representing TiO_2/FeO ratio and the oblique lines representing common mineral solid-solutions suggest that most of the detrital opaque minerals are ilmenite (with some ilmenite–haematite intergrowths), ferropseudobrookite, and rutile. They are apparently erosional products of the metamorphosed Precambrian gneissic and granitic basement, and are paramagnetic at surface temperature. These phases are not

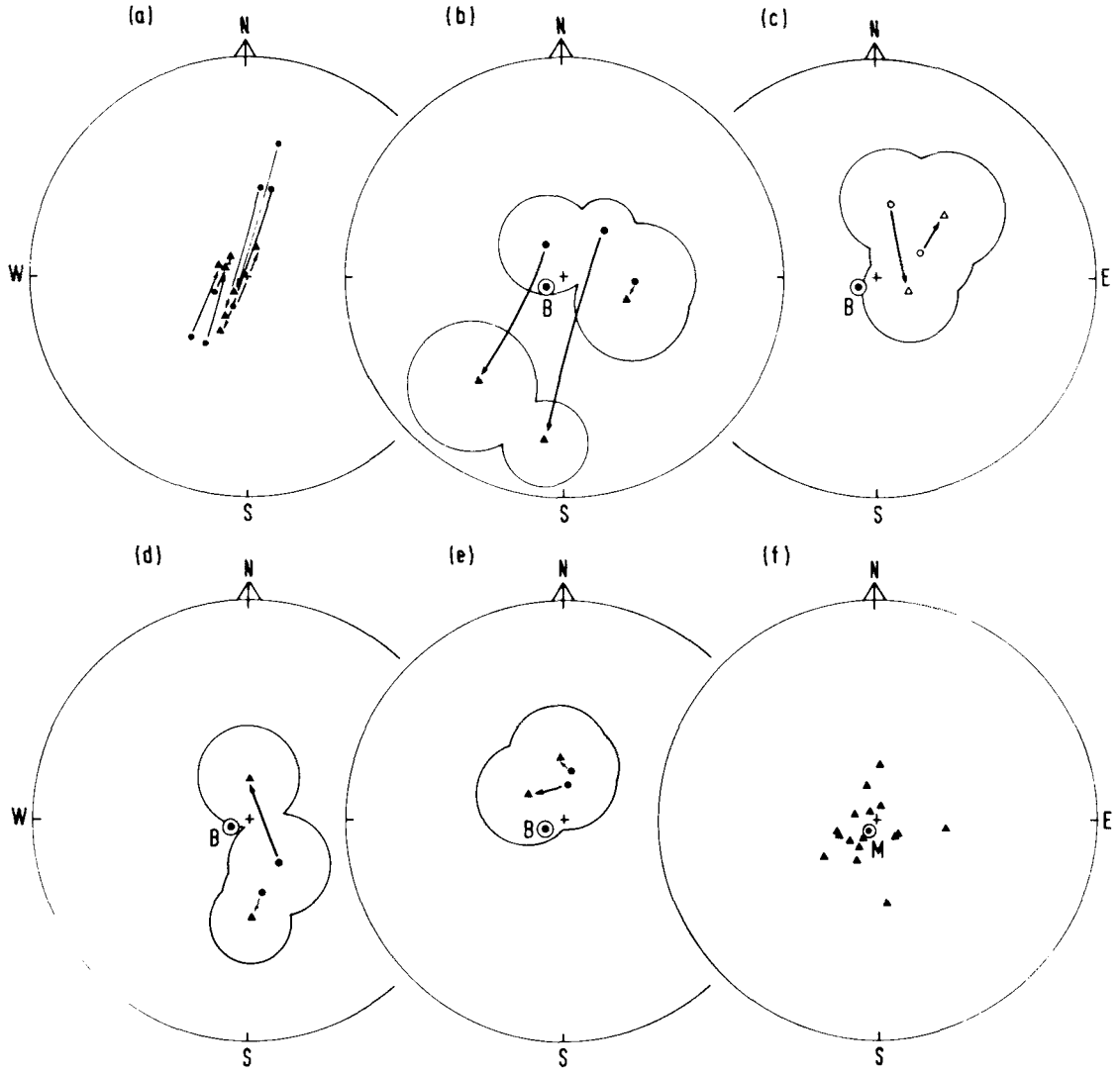

Figure 7. Bedding correction of site-mean directions of the high-temperature component. Data shown in different plots are from: (a) the Carboniferous part of the formation in Davis Gap area; (b) the Late Devonian part of the formation; (c) the Mount Eclipse Syncline; (d) The Walbiri Anticline; (e) the eastern end of the Patmungala Syncline; (f) partial bedding-corrected data of all the sites according to model B. Small solid (open) circles are projections of site-mean directions on the lower (upper) hemisphere before bedding correction. Large circles are projections of the α_{95} cone. Solid (open) triangles are projections of the site-mean directions on the lower (upper) hemisphere after full (a–e) or partial (f) bedding correction. B in (b–e) represents the best grouped mean direction of the Carboniferous section in Davis Gap area calculated according to model B. M in (f) represents the overall mean direction.

considered to contribute to the remanent magnetization. The high-Fe opaque mineral grains at site EL28 are probably haematite, as suggested by the low magnetization intensity and high unblocking temperature of these samples. However, the uncommon nature of these detrital haematite grains in the Ngalia samples makes them unlikely to be the carriers of the consistent high-temperature magnetic remanences.

5.2 Type B, red coatings on the detrital quartz grains

This type of iron-rich mineral occurs mainly in samples from the eastern hinge of the Patmungala Syncline, and in a few sites in the Mount Eclipse Syncline. Whether these red coatings are haematite, or not, could not be determined with confidence. Even if they are, the following arguments suggest that they are unlikely to be carrying any pre-deformational magnetic remanence, and may not be the carriers for the high-temperature characteristic remanence: (1) because the boundaries between quartz grains in the Davis Gap samples, as well as some samples from other areas, are generally quite clean, this type of magnetic carrier cannot be responsible for the remanence in these samples; (2) because undulatory optical extinction in the silica cement and quartz overgrowths enclosing the red coating are common, and in some samples the red coatings are found to have been deformed between quartz grains during pressure solution (Figs 9c,d), we believe that the red coatings have suffered the main phase of grain-scale deformation; and (3) if the characteristic remanence were carried by these pre-deformational red coatings, then according to the passive marker hypothesis (e.g. Van der Pluijm 1987) the

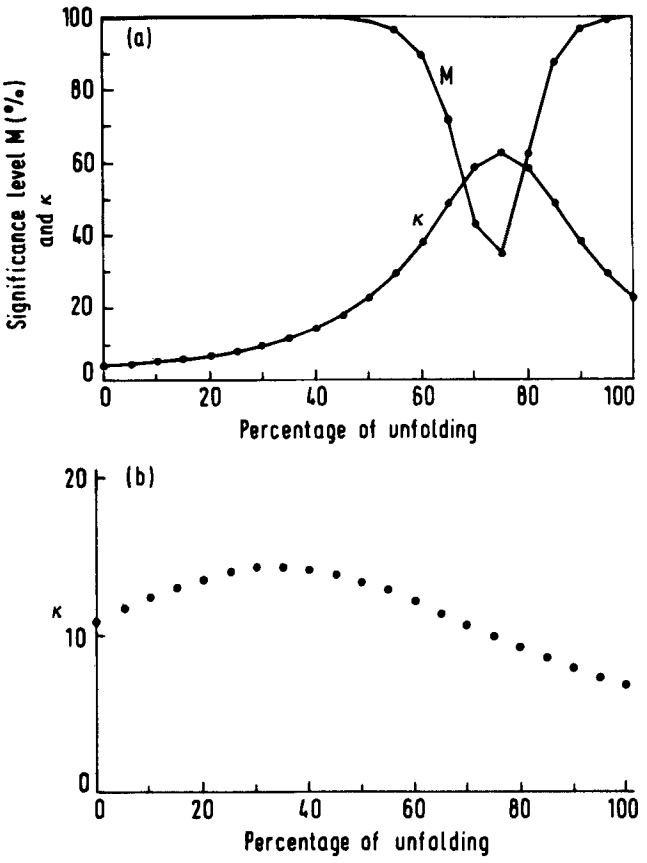

Figure 8. Change of McFadden & Jones' (1981) significance level (M) and the Fisher precision parameter (k) during stepwise 'unfolding' of the high-temperature component. (a) 'Unfolding' of data from Sites EL01, 05, 06, 07, 29, 30, 31 from the Davis Gap area. (b) 'Unfolding' of data from all the other sites in combination with the least dispersed (75 per cent 'unfolded') data from the Davis Gap area according to model B.

remanent direction in the Early Carboniferous samples from the hinge of the Patmungala Syncline (sites EL22–EL24 in Fig. 1b), in which the red coatings are abundant, should not have been as strongly affected by the internal strain as were the directions from the samples from the limbs. We would thus expect to find earliest Carboniferous primary directions from the hinge samples. However, as shown in Fig. 7(e), the site-mean directions from these samples are as steep as samples from elsewhere, and do not correspond to the anticipated shallow inclination derived from the Australian APWP (Li *et al.* 1988). Therefore, if these coatings contribute at all to the characteristic remanent magnetization, it is probably remanence acquired after the pressure solution along quartz-grain boundaries during the folding.

5.3 Type C, red pigment around iron-rich minerals

Red to dark brown pigment occurs either as cryptocrystalline and amorphous iron oxides around weathered iron-rich minerals (mainly biotite, Fig. 9e, f), or as pigment filling the voids between detrital grains. Since this type of Fe-rich material is the only possible magnetic carrier we can identify from the samples in the Davis Gap area, and in some of the samples from other areas, we deduce that it is haematite. Although the pigment also carries magnetization formed during recent weathering, as the intensity of this recent component is mostly very low relative to the characteric high-temperature component, the relative proportion of the recent-component carrier is inferred to be small.

As shown in Section 4, the high-temperature remanent magnetization in the Davis Gap area is not a post-folding overprint, so the magnetic carriers cannot be younger than the deformation. Moreover, as most of this very fine-grained haematite occurs around altered detrital grains only, and its distribution is not restricted to the deformed quartz-grain boundaries (as for pre-deformational haematite coating),

Table 3. Mean directions and palaeomagnetic poles calculated according to different 'unfolding' models

	Lower Carboniferous Rocks in the Davis Gap Area Only (Sites EL01,05,06,07,29,30,31)					Combined Davis Gap Results (75% 'unfolded') with Data from all the Other Accepted Sites in both Upper Devonian and Lower Carboniferous Rocks									
Model	D	I	N	k	α_{95}	D	I	N	k	α_{95}	% of 'un-folding'*	The South Pole Lat. (°S)	Long. (°E)	dp (°)	dm (°)
A.	273.6	82.6	7	62.3	7.7	221.9	85.3	16	14.2	10.1	30	29.1	124.2	19.9	20.1
B.	244.8	80.0	7	55.3	8.2	215.5	82.6	16	14.3	10.1	35	33.8	121.2	19.2	19.7
C.	222.5	71.8	7	41.5	9.5	209.4	78.2	16	13.2	10.6	35	41.4	116.7	18.8	19.9
D.	333.4	79.9	7	73.1	7.1	283.6	88.1	16	13.2	10.5	30	21.4	127.3	20.9	21.0

* – 'unfolding' of other accepted sites. S = the southern limb; N = the northern limb. Dashed lines represent bedding before bedding-correction. Thick solid lines represent bedding after bedding-correction. Fine solid lines represent the horizontal plane.

Note: The south pole position for the preferred model B calculated from Davis Gap data alone is (29.2°S, 110.9°E) with dp=15.0°, dm=15.7°. The 95% error oval of this pole largely overlaps that of the south pole calculated using all accepted sites.

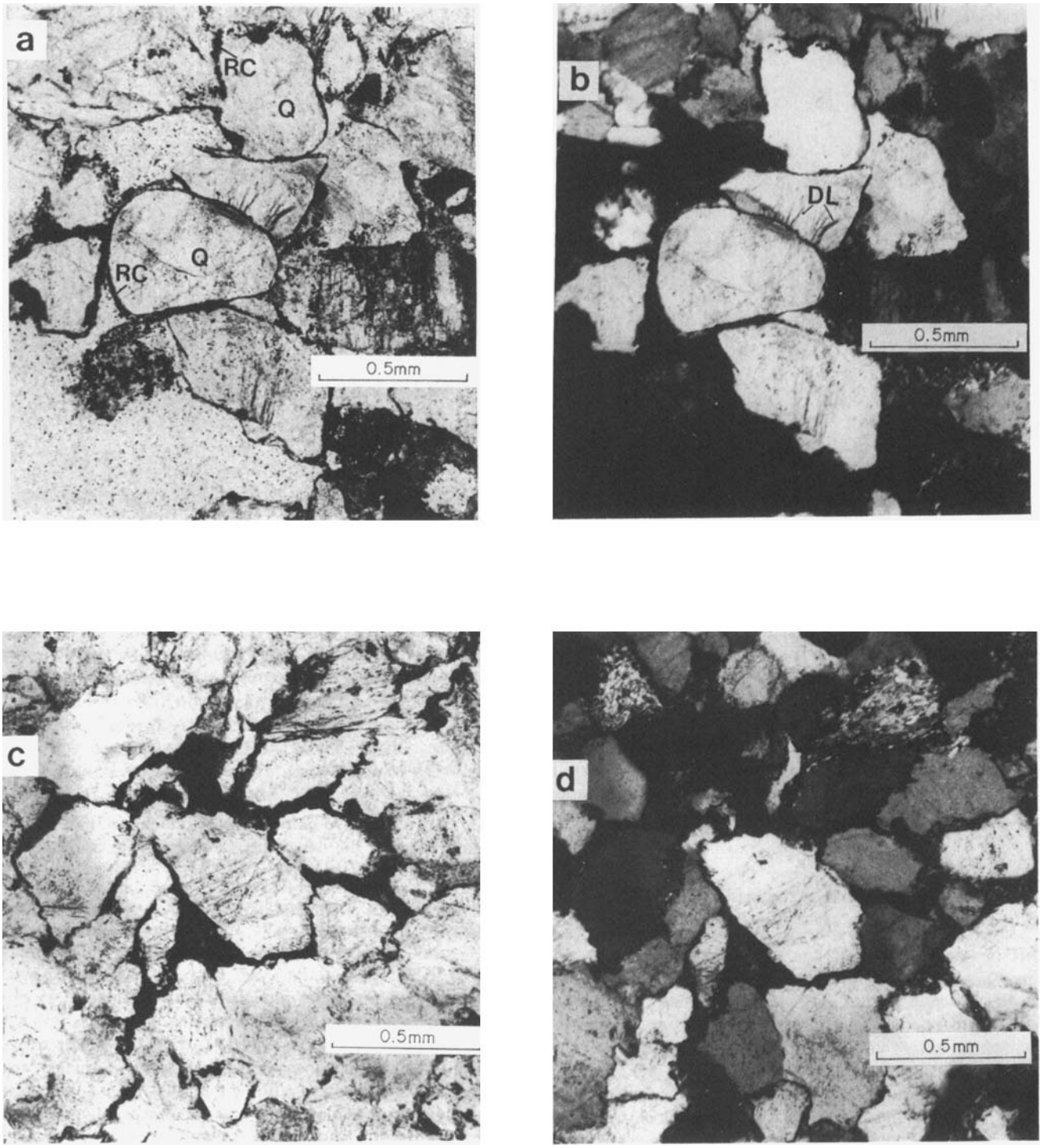

Figure 9. Photomicrographs showing: (a) and (b), detrital quartz grains (Q) with pre-deformational red coatings (RC), and deformation lamellae in quartz grains (DL) (sample EL04C); (c) and (d), pre-deformational red coatings deformed during pressure-solution suturing of quartz-grain boundaries (dark material on the plane-light photograph. Some of the large patches of dark material could also belong to type C iron-oxide. Photos taken from sample EL31H); (e) and (f): red pigment around iron-rich minerals (sample EL06I). Photographs (a), (c) and (e) are taken under plane-polarized light, and (b), (d) and (f) are under cross-nicols.

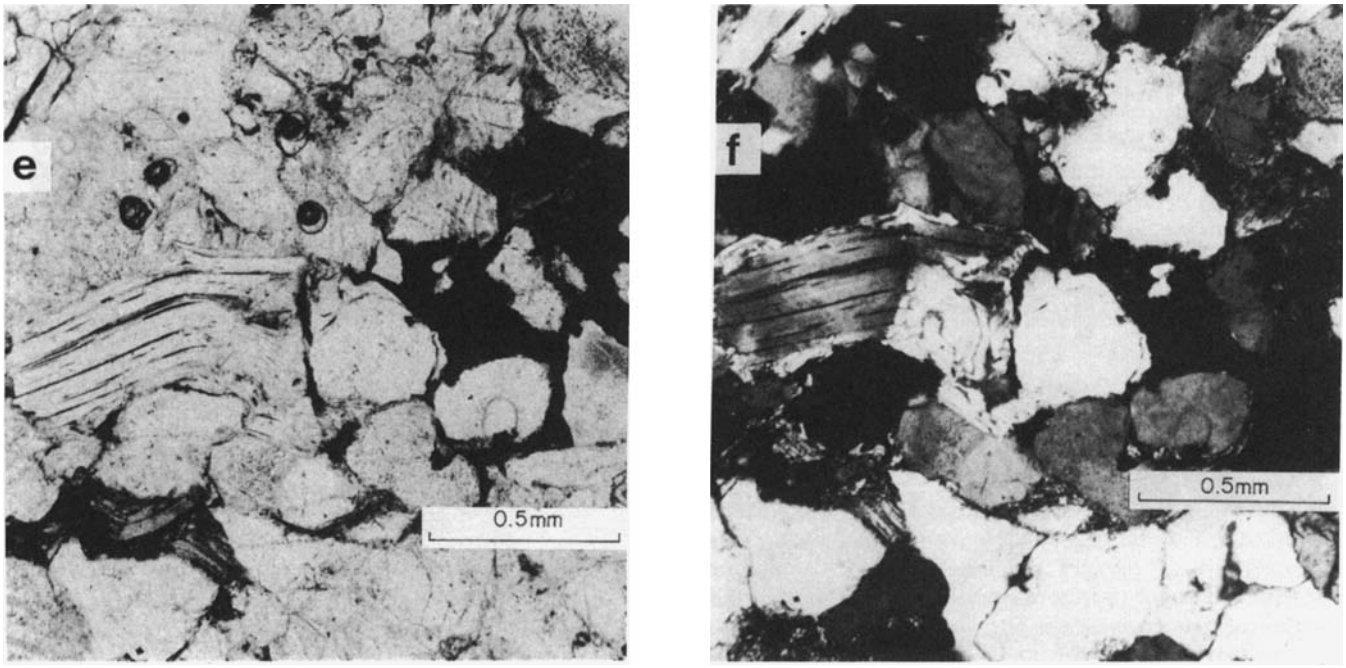

Figure 9. (e) and (f) (see previous page).

the red pigment is likely to have formed during the deformation.

5.4 Conclusion

In summary, this brief petrographic study indicates that the consistent high-temperature remanence in the rocks is unlikely to be a pre-deformational remanent magnetization affected by later penetrative deformation (e.g. Van der Pluijm 1987). Rather, the petrography suggests a syn-deformational, possibly chemical origin for the characteristic remanence.

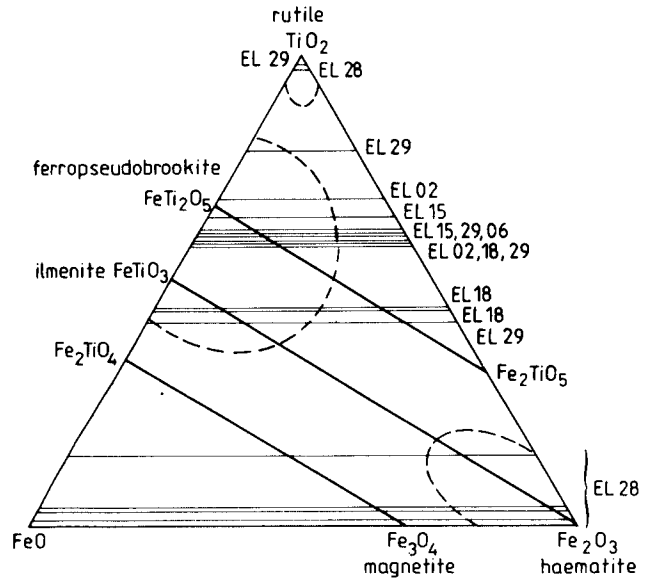

Figure 10. Ternary diagram showing the chemical composition of the detrital opaque minerals. Oblique lines represent the common mineralogy solid solutions. Horizontal lines show the measured TiO/FeO ratios of the detrital opaque minerals. Areas surrounded by dashed lines give the inferred mineralogy.

6 DISCUSSION

6.1 Age of the syn-deformational remanence and its significance for the development of the Alice Springs Orogeny (ASO)

The usefulness of palaeomagnetic data largely relies on the precision of their determination and the accuracy of their palaeohorizontal and age. In this study, the palaeohorizontal of the bedding in the Davis Gap area is bounded by the two extreme 'unfolding' models, C and D (Table 3). A more realistic estimate of the development of bedding attitudes probably corresponds to model B, which is consistent with local structural evidence and intermediate between models C and D. Moreover, although model A is different in principle from model B, in practice the best-fit interpretation of the data is not significantly different. Palaeomagnetic poles calculated according to the different models are listed in Table 3.

The age of this palaeomagnetic pole directly relates to the age of the deformation, which post-dates deposition of the uppermost part of the Mount Eclipse Sandstone. Although Wells & Moss (1983) assigned a Late Carboniferous age to the top part of the formation, the reliability of such an age, determined from plant fossils, is uncertain. The fossils in question are macrofossils, from a relatively isolated outcrop with evidently low bedding inclination in the western part of the basin (22.4°S, 130.9°E, Wells & Moss 1983, appendix 6). Even if those fossils are Late Carboniferous, some doubt

exists as to whether they are part of the folded Ngalia Basin succession or younger deposits of the Innamincka regime (Veevers 1984).

A more reliable age determination from spore assemblages from the middle part of the formation indicate a Visean age (R. Evans, G. Playford & E. Truswell in Saucier 1981, unpublished work; D. G. Morris, pers. comm.). Thus, the top part of the formation could extend well into mid-Carboniferous (Namurian) (Powell & Veevers, 1987). This provides an older limit for the age of the deformation at about 330 Ma. On the other hand, the age of the Alice Springs Orogeny (ASO) could be 320 ± 10 Ma, as determined by the Rb-Sr method in the Arunta Block south of the basin (Mortimer, Cooper & James 1987; older data summarized in Powell & Veevers 1987). Thus, a mid-Carboniferous age can be assigned to the deformation of the Mount Eclipse Sandstone, and this date is taken as the age of the palaeomagnetic pole. The predominant reversed polarity of the remanences is consistent with this age assignation.

ASO-related magnetic overprints have also been reported in the Arunta Block and the Amadeus Basin, just south of the Ngalia Basin. McWilliams (1977) discovered overprint components from the Adelaidean Areyonga Formation and Pertatataka Formation at Ellery Creek and in the NE part of the Amadeus Basin. He interpreted these overprints as being acquired during, or just after, the ASO. Kirschvink (1978) reported a steep downward overprint from the Precambrian and Cambrian rocks at the Ross River section, in the NE Amadeus Basin. He interpreted that overprint as being acquired shortly before or during the ASO. Klootwijk (1980) also found an ASO-related overprint in the Cambrian rocks at Areyonga and at Ross River, in the Amadeus Basin. He interpreted that overprint as being of pre-folding origin.

To interpret the discrepancy in the ages of the ASO-related overprints, Klootwijk (1980) and Kirschvink (1978, pers. comm. in Klootwijk 1980) invoked a geographic difference in the timing of the main folding phase. However, if we plot all the possible palaeomagnetic poles calculated from both the *in situ* and bedding-corrected ASO-related remanences, we find that these poles are greatly dispersed before bedding correction, but cluster close to the poles EL(A) and EL(B) from the Mount Eclipse Sandstone after bedding correction. Their best grouping could probably be obtained during the later stage of the bedding correction (Fig. 11). A pole calculated from the stable remanences measured in the Attutra Metagabbro and its contiguous amphibolite (Whiting 1986) also falls not far from this group of poles (Fig. 11). Although Whiting originally interpreted this magnetization as of Proterozoic age, its steep downward and reversed direction coupled with the intensity of the ASO suggests it could also be an ASO-related overprint. Thus, we believe that all the ASO-related remanences in the Amadeus Basin and in the Arunta Block were probably acquired after the initiation of the folding, at about the same time as the acquisition of the syn-deformational remanence in the Mount Eclipse Sandstone of the Ngalia Basin (i.e. at about 320 ± 10 Ma). The main phase of folding (and maybe the thrusting as well) in the NE Amadeus Basin probably occurred at about the same time as that in the Ngalia Basin, which was during the mid-Carboniferous.

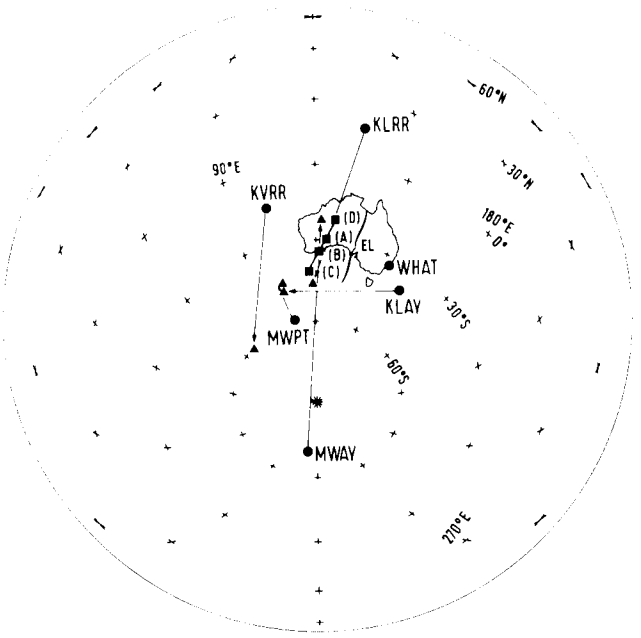

Figure 11. Equal-area projection of the ASO-related overprint poles from central Australia. Squares are poles obtained by this study, with poles A, B, C, and D representing models A–D. Circles (except pole WHAT) are *in situ* poles from the Amadeus Basin, and the connected triangles are the bedding-corrected poles. MWAY and MWPT are overprint poles obtained from the Areyonga Formation and the Pertatataka Formation, respectively (McWilliams 1977). KVRR is the overprint pole obtained from the Ross River section by Kirschvink (1978). KLRR and KLAV are the overprint poles obtained by Klootwijk (1980) from the Ross River section and the Areyonga section, respectively. The WHAT pole is obtained from the Attutra Metagabbro and its contiguous amphibolite, Arunta Block (Whiting 1986).

6.2 About the mechanism for the widespread Permo-Carboniferous magnetic overprint

As first realized by Creer and his colleagues (e.g. Creer 1968), there is a widespread magnetic overprint over Europe and North America during the Late Palaeozoic Kiaman interval. Courtillot *et al.* (1986) summarized that such an overprint has been confirmed by many studies of Laurasia, Baltica, Armorica and northern Gondwanaland. The discovery of the syn-deformational remanence in this study extends the evidence for this overprint event to eastern Gondwanaland. Creer (1968) and Irving & Strong (1985) suggested that the widespread overprint was the result of prolonged deep tropical weathering. However, Miller & Kent (1986) argued that since North America had been in a near-equatorial position until the Late Permian and the overprint only occurred during the Permo-Carboniferous folding, the overprint seems to be more related to orogenic events rather than the palaeolatitude of the continent. The widely reported syn-deformational remanent magnetizations (see 4.1), many of which are Hercynian in age, and the appearance of the polar region overprint in this study, support Miller & Kent's argument. It is likely to be the onset of the climax of the Hercynian orogenies, which is

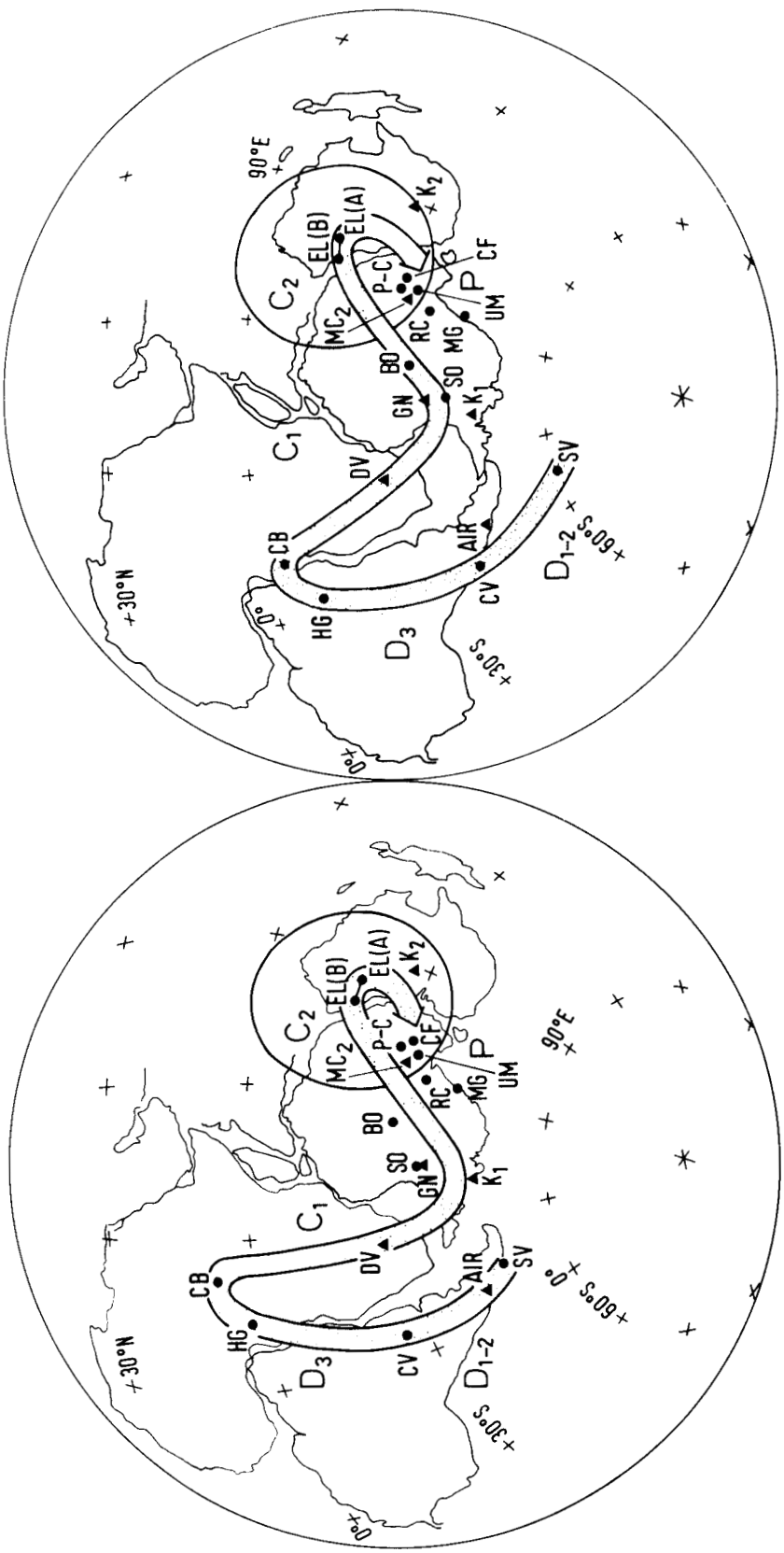

Figure 12. Equal-angle projection of selected Late Palaeozoic palaeomagnetic pole positions and the suggested apparent polar wander path for Gondwanaland. (a) Smith & Hallam (1970) palaeogeographic construction, (b) Scotese *et al.*, (1987, work in progress) palaeogeographic construction. Dots represent poles from Australia, and triangles poles from Africa. EL(A) and EL(B) are poles obtained from the Mount Eclipse Sandstone according to interpretation models A and B. AIR, Silurian ring complex, Western Africa (Hargraves, Dawson & Van Heuten 1987); SV, Snowy River Volcanics, Lachlan Fold Belt (LFB) (Schmidt *et al.* 1987); CV, Comerong Volcanics, LFB (Schmidt *et al.* 1986); HG, Hervey Group sandstone, LFB (Li *et al.* 1988); CB, Canning Basin limestone, Western Australia (Hurley & Van der Voo 1987); DV, Dwyka glacial varves, Central Africa (McElhinny & Opdyke 1968); K1 and K2, K3 redbeds, eastern Africa (McElhinny & Opdyke 1968); GN, Gneiguira Supergroup, Western Africa (Kent *et al.* 1984); SO, post-folding overprint from the Snowy River Volcanics (Schmidt *et al.* 1987); BO, post-folding overprint from the Buchan Caves limestones, LFB (Schmidt *et al.* 1987); CF, MG, RC, Late Carboniferous Rocky Creek Formation, Main Glacial Stage, and Currabubula Formation, LFB (Irving 1966). P–C, Permo-Carboniferous volcanics, New England Fold Belt (McElhinny & Embleton 1974); UM, Upper Marine latites, LFB (Irving & Parry 1963). MC2, the mean Permian pole from Africa (Martin *et al.* 1978). The 95 per cent confidence oval for the EL(B) pole is shown.

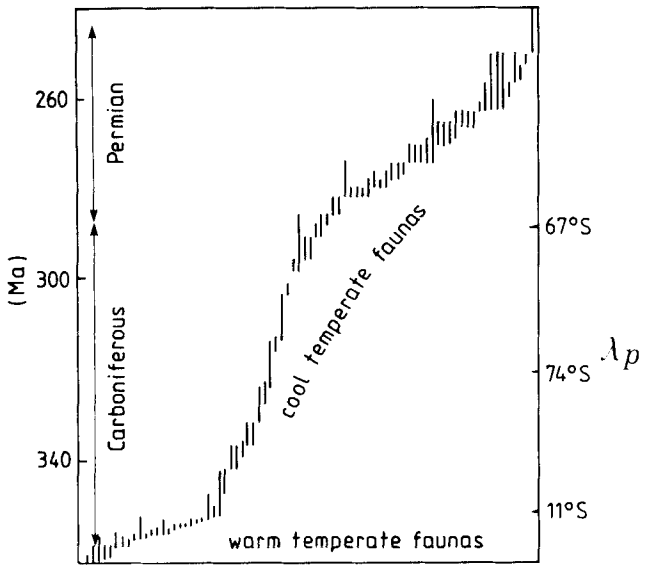

Figure 13. Stratigraphic ranges of marine invertebrate faunas recognized in the Australian Late Palaeozoic successions (after Runnegar & Campbell 1976). The palaeolatitudes (λp) calculated for Central Australia (Alice Springs) according to the APWP in Fig. 12(b) are also shown.

probably related to the collision of Laurussia and Gondwanaland (see 6.3), that could have changed the thermochemical, as well as the mechanical conditions of the rocks, and thus caused widespread Permo-Carboniferous overprinting. Nevertheless, we believe that worldwide Late Palaeozoic overprinting would not have been so well recognized had it not happened during the prolonged Kiaman reversal interval.

6.3 The fast southward movement of eastern Gondwanaland, and the formation of Palaeozoic Pangaea

Palaeomagnetic poles for the Mount Eclipse Sandstone, calculated according to models A and B as listed in Table 3, are plotted in Fig. 12, together with selected Late Palaeozoic palaeomagnetic poles for both Australia and Africa, which are either class A or class B poles, according to the Briden & Duff (1981) scheme.

The EL(B) pole places Central Australia at a palaeolatitude of 75° ± 20°S during the mid-Carboniferous. But the early Late Devonian pole (pole CV from Schmidt *et al.* 1986) and latest Devonian–Early Carboniferous poles (pole CB from Hurley & Van der Voo 1987, and pole HG from Li *et al.* 1988) all indicate a low palaeolatitude (10°–15°S) for central Australia. Thus, eastern Gondwanaland appears to have moved rapidly southward by 60 ± 20° in the Early Carboniferous times, between 350 and 320 Ma. The latititudinal speed required for such a movement ($2° Ma^{-1}$) is more than double the maximum, absolute, half-rate of present seafloor spreading, but similar in rate to the rapid northward motion of India in Late Cretaceous times (Sclater & Fisher 1974). The large overlap of the EL poles and the existing Late Carboniferous–Early Permian poles suggests that after that fast movement, eastern Gondwanaland stayed close to the south pole until the Early Permian. This conclusion is in very good agreement with palaeontological evidence (Runnegar & Campbell 1976), which shows that diverse tropical or warm temperate faunas dominated in eastern and NE Australia during the earliest Carboniferous, but the biota suddenly became less diverse in the mid-Carboniferous, and cool-temperate provincial faunas developed during that time and dominated in the Permian (Fig. 13).

While eastern Gondwanaland moved southward, western Gondwanaland (North America and Africa) moved northward towards the palaeo-equator. As shown in Fig. 14a, by mid-Carboniferous times, the northern margin of western Gondwanaland could have moved as far north as about 15° ± 20°N. At that time, the southern margin of the Laurussia was located at around 15° ± 5°S (Kent & Opdyke 1985; older data as summarized by Scotese *et al.* 1984). Therefore, if there was really a face-to-face collision between the two super-continents during mid-Late Carboniferous, as suggested by structural evidence (e.g. Lefort & Van der Voo 1981), the Palaeozoic Pangaea might have been formed as early as mid-Carboniferous, although a palaeogeographic reconstruction based on the above palaeomagnetic data will cause a significant overlap between the two super-continents. By then, the wide ocean separating the two super-continents before the Early Carboniferous (e.g. Hurley & Van der Voo 1987; Li *et al.* 1988) should have been closed, and the Appalachian–Hercynian Orogenic Belt been formed. The overlap in the palaeomagnetic reconstruction could be caused either by the insufficient palaeomagnetic data, or by the possible existence of a long-term zonal non-dipole field. The precision of the present data does not enable us to test which of the previously suggested models (e.g. Pangaea A1 of Wegener 1924; Pangaea A2 of Van der Voo & French 1974; and Pangaea B of Irving 1977, see Fig. 14b–d) is more accurate.

Alternatively, allowing for the indeterminancy of longitude by palaeomagnetic data, there may have been an oblique collision between the two super-continents during mid-Carboniferous times. The two super-continents may have joined either as suggested by Smith, Hurley & Briden (1981) (Fig. 14e), or as shown in Fig. 14a. Both palaeomagnetic and geological data are needed to refine the palaeoreconstruction.

ACKNOWLEDGMENTS

This work was supported by ARGS grant E83 15504, Macquarie University, and funds from CSIRO and the Chinese State Education Commission. We sincerely thank B. J. J. Embleton, D. A. Clark and L. J. Pesonen for their constructive reading of the early script. We also thank D. G. Morris and C. T. Klootwijk for information on the Ngalia Basin, J. Guo for his help in the microprobe analysis, and M. Huddleston for his able assistance in the field.

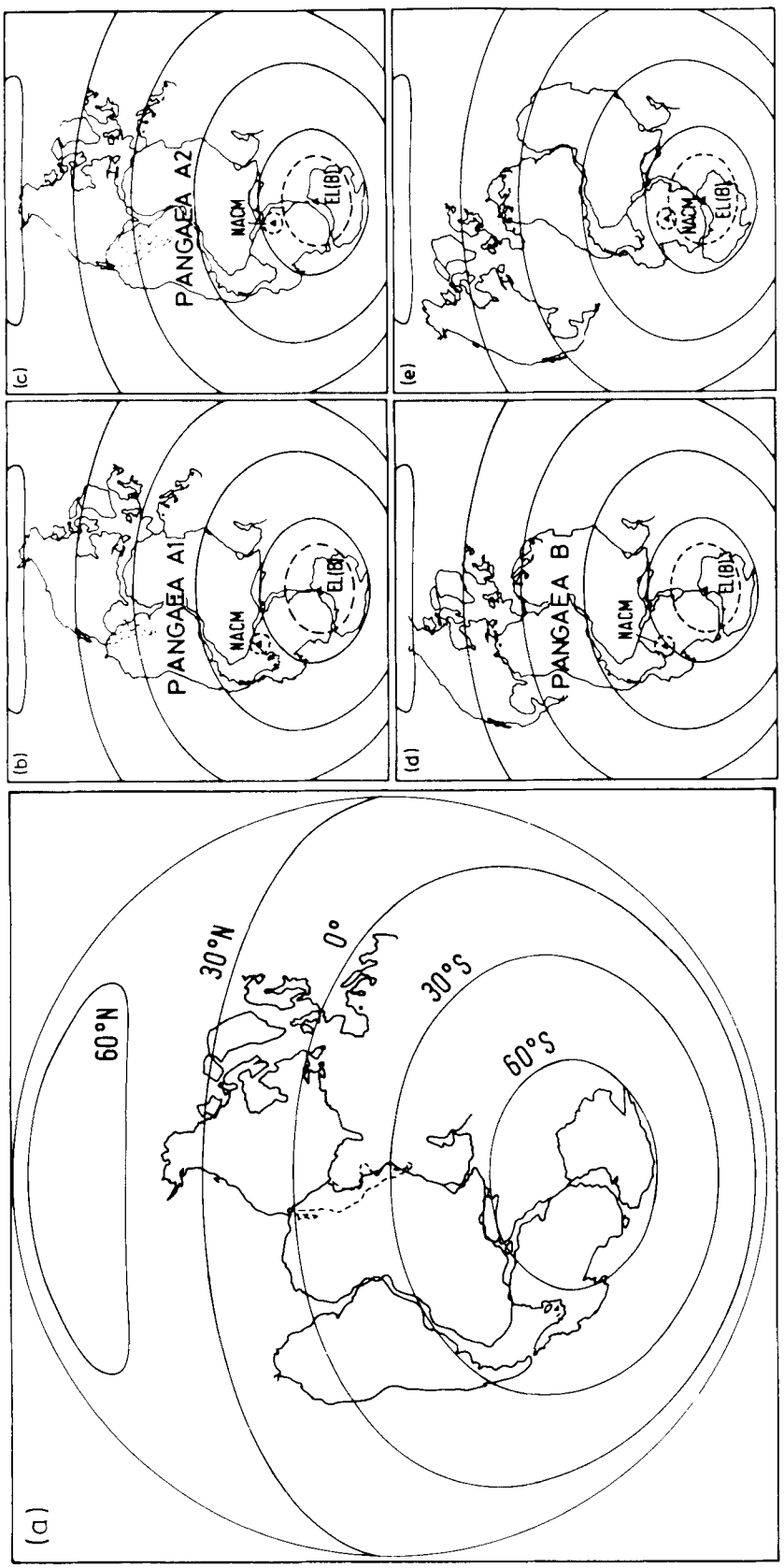

Figure 14. Possible palaeoreconstructions between Gondwanaland and Laurussia during the Late Palaeozoic. (a) shows the palaeolatitudes of the two super-continents during the mid-Carboniferous. Gondwanaland is plotted according to the EL(B) pole of this study. Laurussia is plotted according to the mean mid-Carboniferous North America pole (pole NACM), which is calculated using the 310–330 Ma Canadian Maritime poles as summarized in Scotese *et al.* (1984), and the pole based on the primary remanence in the Mauch Chunk Formation (Kent & Opdyke 1985). In (b)–(e), the palaeolatitudes of Gondwanaland are the same as in (a). The relative positions of Laurussia are according to: (b) Wegener (1924); (c) Van der Voo & French (1974); (d) Irving (1977); (e) Smith *et al.* (1981). The 95 per cent error ovals of the poles EL(B) and NACM are shown as dashed circles. Lambert equal-area projection.

REFERENCES

Briden, J. C. & Duff, B. A., 1981. Pre-Carboniferous paleomagnetism of Europe north of the Alpine Orogenic Belt, in *Paleoreconstruction of the Continents,* Geodyn. Ser. Am. geophys. Un., **2,** 106–114, eds. McElhinny, M. W. & Valencio, D. A.

Caputo, M. V. & Crowell, J. C., 1985. Migration of glacial centers across Gondwana during Paleozoic Era, *Geol. Soc. Am. Bull.*, **96,** 1020–1036.

Chamalaun, F. H. & Porath, H., 1968. Palaeomagnetism of Australian hematite ore bodies, I. The Middleblack Ranges of South Australia, *Geophys. J.*, **14,** 451–462.

Courtillot, V., Chambon, P., Brun, J. P. & Matte, P., 1986. A magnetotectonic study of the Hercynian Montagne Noire (France), *Tectonics,* **5,** 753–767.

Coward, D. A., Cripps, G. S., Maher B. C. & Ridley B. H., 1985. Zero magnetic field furnace controller, CSIRO Division of Mineral Physics, 1983/1984 *Biennial Report,* p. 26.

Creer, K. M., 1968. Palaeozoic palaeomagnetism, *Nature,* **219,** 246–250.

Crowell, J. C., 1978. Gondwanan glaciation, cyclothems, continental positioning, and climate change, *Am. J. Sci.,* **278,** 1345–72.

Facer, R. A., 1983. Folding, strain and Graham's fold test in palaeomagnetic investigations, *Geophys. J. R. astr. Soc.,* **72,** 165–171.

Fisher, R. A., 1953. Dispersion on a sphere, *Proc. R. Soc. A,* **217,** 295–305.

Graham, J. W., 1949. The stability and significance of magnetism in sedimentary rocks, *J. geophys. Res.,* **54,** 131–167.

Granirer, J. L., Burmester, R. F. & Beck, M. E., Jr, 1986. Cretaceous paleomagnetism of the Methow–Pasayten Belt, Washington, *Geophys. Res. Lett.,* **13,** 733–736.

Hargraves, R. B., Dawson, E. M. & Van Houten, F. B., 1987. Palaeomagnetism and age of mid-Palaeozoic ring complexes in Niger, Western Africa, and tectonic implications, *Geophys. J. R. astr. Soc.,* **90,** 705–729.

Hurley, N. F. & Van der Voo, R., 1987. Paleomagnetism of Upper Devonian reefal limestones, Canning Basin, Western Australia, *Geol. Soc. Am. Bull.,* **98,** 138–146.

Irving, E., 1966. Paleomagnetism of some Carboniferous rocks from New South Wales and its relation to geological events, *J. geophys. Res.,* **71,** 6025–6051.

Irving, E., 1977. Drift of the major continental blocks since the Devonian, *Nature,* **270,** 304–309.

Irving E. & Parry, L. G., 1963. The palaeomagnetism of some Permian rocks from New South Wales, *Geophys. J.*, **7,** 395–411.

Irving, E. & Strong, D. F., 1985. Paleomagnetism of rocks from Burin Peninsula, Newfoundland: hypothesis of Late Paleozoic displacement of Acadia Criticized, *J. geophys. Res.,* **90,** 1949–1962.

Kent, D. V., Dia, O. & Sougy, J. M. A., 1984. Paleomagnetism of lower-middle Devonian and Upper Proterozoic-Cambrian (?) rocks from Mejeria (Mauritania, West Africa), in *Plate Reconstruction from Paleozoic Paleomagnetism,* Geodyn. Ser., vol. 12, pp. 99–115, eds Van der Voo, R., Scotese, C. R. & Bonhommet, N.

Kent, D. V. & Opdyke, N. D., 1985. Multicomponent magnetizations from the Mississippian Mauch Chunk Formation of the Central Appalachians and their tectonic implications, *J. geophys. Res.,* **90,** 5371–5383.

King, L. C., 1962. *The Morphology of the Earth,* p. 699, Oliver and Boyd, Edinburgh.

Kirschvink, J. L., 1978. The Precambrian–Cambrian boundary problem: paleomagnetic directions from the Amadeus Basin, central Australia, *Earth planet. Sci. Lett.,* **40,** 91–100.

Kirschvink, J. L., 1980. The least-squares line and plane and the analysis of palaeomagnetic data, *Geophys. J. R. astr. Soc.,* **62,** 699–718.

Klootwijk, C. T., 1980. Early Palaeozoic palaeomagnetism in Australia, *Tectonophysics,* **64,** 249–332.

Kodama, K. P., 1986a. The effect of deformation on the fold test, *Eos Trans. Am. geophys. Un.,* **67,** 268.

Kodama, K. P., 1986b. Effect of flexural slip on Fisherian distributions: implications for fold test, *Eos Trans. Am. geophys. Un.,* **67,** 924.

Köppen, W. & Wegener, A., 1924. *Die Klimate der geolischen Vrzeit,* Bornträger, Berlin.

Lefort, J. P. & Van der Voo, R., 1981. A kinematic model for the collision and complete suturing between Gondwanaland and Laurussia in the Carboniferous, *J. Geol.,* **89,** 537–550.

Li, Z. X., Schmidt, P. W. & Embleton, B. J. J., 1988. Paleomagnetism of the Hervey Group, central New South Wales, and its tectonic implications, *Tectonics,* **7,** 351–367.

Martin, D. L., Nairn, A. E. M., Noltimier, H. C., Petty, M. H. & Schmidt, T. T., 1978. Paleozoic and Mesozoic paleomagnetic results from Morocco, *Tectonophysics,* **44,** 91–114.

McClelland Brown, E., 1983. Palaeomagnetic studies of fold development and propagation in the Pembrokeshire Old Red Sandstone, *Tectonophysics,* **98,** 131–149.

McElhinny, M. W. & Embleton, B. J. J., 1974. Australian paleomagnetism and the Phanerozoic plate tectonics of Eastern Gondwanaland, *Tectonophysics,* **22,** 1–29.

McElhinny, M. W. & Opdyke, N. D., 1968. Paleomagnetism of some Carboniferous glacial varves from Central Africa, *J. geophys. Res.,* **73,** 689–696.

McFadden, P. L. & Jones, D. L., 1981. The fold test in palaeomagnetism, *Geophys. J. R. astr. Soc.,* **67,** 53–58.

McWilliams, M. O., 1977. Late Precambrian palaeomagnetism of Australia and Africa, *PhD thesis,* Australian National University, Canberra, 138 pp.

Miller, J. D. & Kent, D. V., 1986. Synfolding and prefolding magnetizations in the Upper Pennsylvania: implications for the tectonic history of Acadia, *J. geophys. Res.,* **91,** 12791–12803.

Mortimer, G. E., Cooper, J. A. & James, P. R., 1987. U-Pb and Rb-Sr geochronology and geological evolution of the Harts Range ruby mine area of the Arunta Inlier, central Australia, *Lithos,* **20,** 445–467.

Perroud, H., 1983. Palaeomagnetism of Palaeozoic rocks from the Cabo de Penas, Asturia, Spain, *Geophys. J. R. astr. Soc.,* **75,** 201–215.

Powell, C. McA. & Veevers, J. J., 1987. Namurian uplift in Australia and South America triggered the main Gondwana glaciation, *Nature,* **326,** 177–186.

Runnegar, B. & Campbell, K. S. W., 1976. Late Palaeozoic faunas of Australia, *Earth Sci. Rev.,* **12,** 235–257.

Schmidt, P. W., 1982. Linearity spectrum analysis of multicomponent magnetizations and its application to some igneous rocks from south-eastern Australia, *Geophys. J. R. astr. Soc.,* **70,** 647–665.

Schmidt, P. W. & Embleton, B. J. J., 1985. Prefolding and overprint magnetic signatures in Precambrian (~2.9–2.7 Ga) igneous rocks from the Pilbara Craton and Hamersley Basin, NW Australia, *J. geophys. Res.,* **90,** 2967–2984.

Schmidt, P. W., Embleton, B. J. J. & Palmer, H. C., 1987. Pre- and post-folding magnetization from the Devonian Snowy River Volcanics and Buchan Caves Limestone, Victoria, *Geophys. J. R. astr. Soc.,* **91,** 155–170.

Schmidt, P. W., Embleton, B. J. J., Cudahy, T. J. & Powell, C. McA., 1986. Prefolding and premegakinking magnetization from the Devonian Comerong Volcanics, New South Wales, Australia, and their bearing on the Gondwana pole path, *Tectonics,* **5,** 135–150.

Schwartz, S. Y. & Van der Voo, R., 1984. Paleomagnetic study of thrust sheet rotation during foreland impingement in the Wyoming–Idaho Overthrust Belt, *J. geophys. Res.,* **89,** 10,077–10,086.

Sclater, J. G. & Fisher, R. L., 1974. Evolution of the east central Indian Ocean, with emphasis on the tectonic setting of the Ninetyeast Ridge, *Geol. Soc. Am. Bull.,* **85,** 683–702.

Scotese, C. R., Van der Voo, R., Johnson, R. E. & Giles, P. S., 1984. Paleomagnetic results from the Carboniferous of Nova Scotia, in *Plate Reconstructions from Paleozoic Paleomagnetism,* Geodynamics Ser., **12,** 63–81, eds Van der Voo, R., Scotese, C. R. & Bonhommet, N.

Smith, A. G., Hurley, A. M. & Briden, J. C., 1981. *Phanerozoic Paleocontinental World Maps,* Cambridge University Press, 102 pp.

Spariosu, D. J., Kent, D. V. & Keppie, J. D., 1984. Late Paleozoic motion of the Meguma Terrane, Nova Scotia: new paleomagnetic evidence, in *Plate Reconstructions from Paleozoic Paleomagnetism*, Geodynamics Ser., **12,** 82–98. eds Van der Voo, R., Scotese, C. R. & Bonhommet, N.

Strangway, D. W., Honea, R. M., McMahon, B. E. & Larson, E. E., 1968. The magnetic properties of naturally occurring goethite, *Geophys. J. R. astr. Soc.*, **15,** 345–359.

Torsvik, T. H., Sturt, B. A., Ramsay, D. M., Kisch, H. J. & Bering, D., 1986. The tectonic implications of Solundian (Upper Devonian) rocks of Kvamshesten, western Norway, *Earth planet. Sci. Lett.*, **80,** 337–347.

Van der Pluijm, B. A., 1987. Grain-scale deformation and the fold test–evaluation of syn-folding remagnetization, *Geophys. Res. Lett.*, **14,** 155–157.

Van der Voo, R. & French, R. B., 1974. Apparent polar wandering for the Atlantic-bordering continents: Late Carboniferous to Eocene, *Earth Sci. Rev.*, **10,** 99–119.

Veevers, J. J. (ed.), 1984. *Phanerozoic Earth History of Australia,* Clarendon Press, Oxford, 418 pp.

Veevers, J. J. & Powell, C. McA., 1987. Late Paleozoic glacial episodes in Gondwanaland reflected in transgressive–regressive depositional sequences in Euramerica, *Geol. Soc. Am. Bull.*, **98,** 475–487.

Wegener, A., 1924. *The Origin of Continents and Oceans* (English trans.), Methuen, London, 212 pp.

Wells, A. T. & Moss, F. J., 1983. The Ngalia Basin, Northern Territory: stratigraphy and structure, *BMR Bulletin*, No. 22, 88 pp.

Whiting, T. H., 1986. Aeromagnetics as an aid to geological mapping–a case history from the Arunta Inlier, Northern Territory, *Aust. J. Earth Sci.*, **33,** 271–286.

Zijderveld, J. D. A., 1967. A.C. demagnetization of rocks, in *Methods in Palaeomagnetism*, eds Collinson, D. W., Creer, K. M. & Runcorn, S. K., pp. 254–286, Elsevier, New York.